

## Development of a Low-order Adaptive Optics System at Udaipur Solar Observatory

A. R. Bayanna\*, B. Kumar, R. E. Louis, P. Venkatakrishnan & S. K. Mathew  
*Udaipur Solar Observatory, Physical Research Laboratory, P.O. Box 198, Dewali, Badi Road, Udaipur 313 001, India.*

\*e-mail: bayanna@prl.res.in

**Abstract.** A low-order Adaptive Optics (AO) system is being developed at the Udaipur Solar Observatory and we present in this paper the status of the project, which includes the image stabilization system and calibration of wavefront sensor and deformable mirror. The image stabilization system comprises of a piezo driven tip-tilt mirror, a high speed camera (955 fps), a frame grabber system for sensing the overall tilt and a Linux based Intel Pentium 4 control computer with Red Hat Linux OS. The system operates under PID control. In the closed loop, an rms image motion of 0.1–0.2 arcsec was observed with the improvement factor varying from 10–20 depending on the external conditions. Error rejection bandwidth of the system at 0 dB is 80–100 Hz. In addition to that, we report the on-going efforts in the calibration of lenslet array and deformable mirror for sensing and correcting the local tilt of the wavefront.

**Key words.** Sun: astronomical seeing, adaptive optics, solar telescopes, solar imaging.

### 1. Introduction

A Multi-Application Solar Telescope (MAST) equipped with an Adaptive Optics (AO) system is proposed to be installed at the lake site of Udaipur Solar Observatory (USO) in India. It is planned to build the AO system for high resolution observations in two phases. The first phase involves the development of an image stabilization system (Sridharan *et al.* 2005), which will correct the global tilt of the distorted wave-front and deliver a steady image. The second phase involves correction of local tilts of the residual wavefront using a deformable mirror.

The image stabilization system is in operation and provides an improvement of 10–20 times in the rms image motion. Now, the second phase is in progress. In this paper, we present some of the results we achieved with our image stabilization system and the ongoing efforts for achieving local tilt correction of the wavefront.

## 2. Image stabilization system

### 2.1 Image stabilization system: Global tilt correction

In an image stabilization system, a small portion (typically  $10 \times 10$  arcsec<sup>2</sup>) of a short exposure (typically  $< 10$  ms) image is cross-correlated with a previously recorded reference image. Subsequent images are correlated with the same reference image. The reference image is updated typically every 10 seconds by the best image selected during that period. The cross-correlation extracts the shift of the instantaneous image with respect to the reference image in two orthogonal directions. These shifts are used to feed appropriate voltages to the tip-tilt mirror so that its surface closely approximates the instantaneous global tilt in the wave-front. As the global tilt is removed from the wave-front after being reflected by the tip-tilt mirror, the image motion is arrested. This results in a stable output image in the science camera and thus allows for long exposures.

### 2.2 Description of optical set-up of image stabilization system

The image formed by the 15 cm Coude refractor ( $f/15$  beam) is re-imaged by a combination of two doublets inside the laboratory with a magnification of two. A portion of the image is collimated by a doublet of focal length 200 mm. The collimated beam is reflected by the tip-tilt mirror and another plane mirror and is finally focused by a lens of focal length 300 mm. A beam splitter splits the converging beam equally into two parts: one beam is directed to a ‘science camera’ after passing through a filter of 1 nm bandwidth centered at 430.5 nm and the other beam is directed to the ‘wave-front sensing camera’ after passing through suitable neutral density filters. The final image has a scale of 0.31 arcsec per pixel at the ‘sensing camera’. The light feed and schematic of the optical set-up are shown in Fig. 1.

### 2.3 System components

Apart from optical elements, the main components of the system are: (1) A 16-bit 2-channel digital-to-analog converter board, (2) the piezo-electric stage and its controller, and (3) the data acquisition system which consists of a fast camera (955 fps) and a frame-grabber card. These are similar to those used in the low cost AO system at NSO/Kitt Peak, USA (Keller *et al.* 2003, hereafter KPA).

### 2.4 Software

The AO system software consists of two C-programs that are executed together and share a common memory through inter process communication mechanism. The first one called “the universal tracker” is largely based on the Linux device driver of the frame grabber card provided by *GOM mbH*. The second one called “the control software”, is used to control the various parameters of the system, including PID. At USO, we have modified the aforesaid software developed by KPA to suit our system. The image stabilization system at USO is working with the closed loop update rate  $\approx 1$  kHz. The closed loop correction bandwidth is  $\sim 80$ – $100$  Hz as shown in Fig. 2. The rms image motion in the closed loop is about 0.1 arcsec and is better than that in the open loop operation by a factor of 10–20.

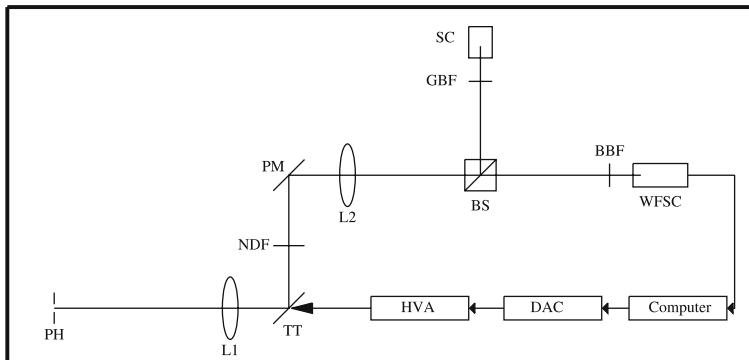


**Figure 1.** Coude telescope (top panel) at the light feed and schematic of the optical set-up (bottom panel) inside the laboratory is shown here. PH: Field stop, L1 and L2: Lenses, PM: Plane mirror, BS: Beam splitter, WFSC: Wavefront sensing camera, SC: Science camera, PC: Control computer, HVA: High voltage amplifier, DAC: Digital to analog converter.

### 3. Correction of local tilt of the wavefront

Correction of the local tilt of the wavefront involves two important steps, the first one being sensing the local tilts and second one is correction. We employ Shack-Hartmann Wavefront Sensing (SHWFS) using a lenslet array ( $9 \times 9$  lenslets or sub-apertures) and a 37-channel micro-machined membrane mirror (DM) for correction. The pitch and the focal length of the lenslet array are  $600 \mu\text{m}$  and  $145 \text{ mm}$ , respectively. This pitch size of lenslet array and CCD allows us to accommodate only 17 sub-apertures in the sensing camera. The code for calculating the local tilts of the wavefront using the lenslet array has been successfully tested (Bayanna *et al.* 2005). The DM and lenslet array were characterized through lab simulations before being used for solar observations. An optical set-up was made using a He-Ne laser source inside the lab. Using suitable lenses and apertures, we obtained a  $15 \text{ mm}$  collimated beam from the laser source. Two similar DMs were employed in the set-up to use one of them as a source of distortion and the other as a correcting element. However, in this paper

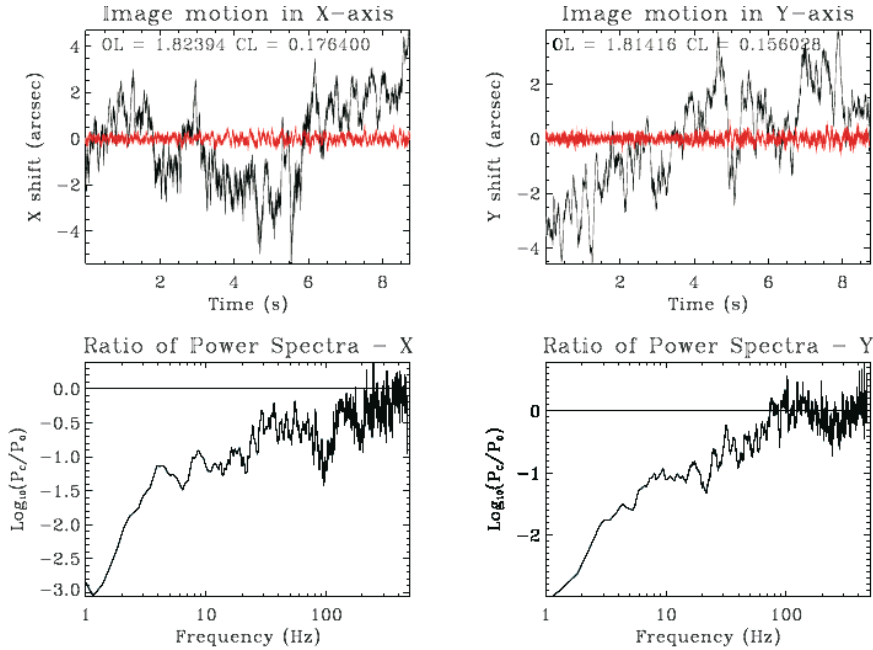


**Figure 2.** Top panels show image motion in the open loop (OL) and closed loop (CL) in black and red, respectively. Bottom panels show the ratio of power spectra of closed to open loop. P and D control parameters have been used in tuning the system. The values for *Channel 0* are:  $P_0 \approx 20$  and  $D_0 \approx 80$  and that for *Channel 1* are:  $P_1 \approx 0.45P_0$  and  $D_1 \approx 0.45D_0$ .

we are presenting the calibration details only, which has been completed. Before calibrating the DM, mapping of the actuator space with the sub-aperture space was carried out, so that the distortion could be created at the desired location and in a systematic manner. The main purpose of the calibration was to estimate the influence matrix of the deformable mirror, i.e., how a change in voltage given to a particular actuator affects the change in shift in all the sub-apertures. Voltage was applied to each actuator of the DM from 0–225 DACs and the corresponding image motion in each sub-aperture was recorded. The slopes of voltage vs. shift curves for all the sub-apertures were estimated. The same procedure was repeated for all the actuators. The influence matrix is a rectangular matrix of size  $2M \times N$ , with the number of columns equal to the number of actuators ( $N$ ) and the number of rows equal to the number of slope measurements ( $2M$ ), which is twice the number of sub-apertures. The matrix is inverted using Singular Value Decomposition. As we have 17 sub-apertures and 37 actuators, to have practical and best suited solutions by inverting the influence matrix, we restricted our usable actuators to only 7. To check the influence matrix and the code for the estimation of voltages from the shift vector, an arbitrary voltage set was applied to the deformable mirror and the shift vectors along the  $x$ - and  $y$ -directions in the sub-aperture plane were recorded as shown by the solid line in Fig. 3. Using the observed shift vector and the influence matrix, a voltage vector was obtained, which was in agreement with the applied voltage vector. The application of this voltage vector produced nearly the same shift vector as the one corresponding to the applied voltage set. These are shown by the

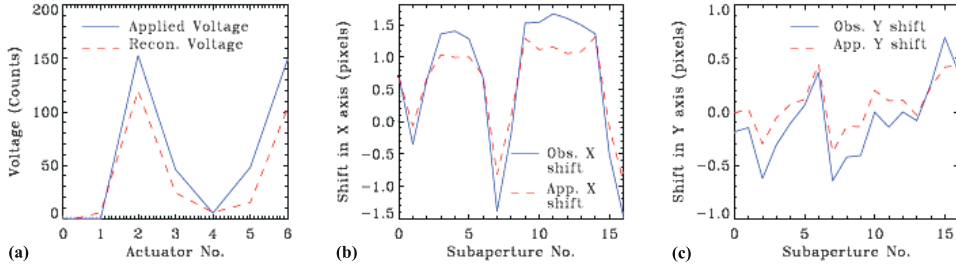


**Figure 3.** (a) Plot depicts voltages applied to the deformable mirror and the reconstructed voltage set obtained from the influence matrix. (b) and (c) Plots depict the shift obtained for a given voltage set and the shifts obtained from the reconstructed voltage set along x and y axes respectively.

dashed lines in Fig. 3. During this process, we have observed that in the present optical set-up the DM is insensitive at voltages smaller than 60 DACs. This is why the shift observed and the consequent voltage vector obtained through the influence matrix are very small for low values of applied voltages. We also observed that for the image motion more than 0.5 pixels, the voltage vector obtained is sensitive enough to influence the DM surface. Thus, even if the image motion in one of the sub-apertures due to the local wavefront tilt is above 0.5 pixels, the subsequent voltage vector will be sensitive enough to suppress it to the sub-pixel domain, which is our requirement. The DM is ready for integration with the image stabilization system and for dynamic correction for complete realization of the AO system.

### Acknowledgements

We express our sincere thanks to Dr. R. Sridharan for his involvement in the initial phase of the development of the AO system at USO. We are also thankful to Prof. C. U. Keller for sharing his expertise on AO.

### References

- Bayanna, A. R., Mathew, S. K., Venkatakrishnan, P., Kumar, B., Sridharan, R. 2005, In: *The Proceedings of International Conference on Optics & Optoelectronics*, held at IRDE, Dehradun, India (eds) A. K. Kaul and S. Gupta, p. PP-AO-1.  
 Keller, C. U., Plymate, C., Ammons, S. M. 2003, *SPIE*, **4853**, 351.  
 Sridharan, R., Bayanna, A. R., Kumar, B., Venkatakrishnan, P. 2005, *Bull. Astron. Soc. India*, **33**, 414.